RSC Advances

PAPER

View Article Online
View Journal | View Issue

Cite this: *RSC Adv.*, 2025, **15**, 22546

Insights into the antioxidant activity and metal chelation capacity of natural marine bromophenols: role of C–O–C and C–C linkages and the catechol group†

Houssem Boulebd *

Marine algae are an important source of phenolic compounds with multiple biological applications. Among them, bromophenols (BPs) show remarkable antioxidant activity *in vitro*, although their mechanisms of action remain poorly elucidated. In this study, we used density functional theory (DFT) calculations to explore in detail the antioxidant mechanism of two natural BPs (**BP-I** and **BP-II**), differing only in the bond linking their phenolic groups (C–O–C *vs.* C–C). The results revealed that both compounds are effective $HOO^{\bullet}$ scavengers in lipid media, with respective rate constants of 2.40×10^2 and 1.76×10^3 M^{-1} s^{-1}, the **BP-II** derivative (C–C bond) proving more reactive than its **BP-I** counterpart (C–O–C bond). In aqueous media, their reactivity was comparable with high-rate constants of 1.96×10^9 and 2.04×10^9 M^{-1} s^{-1} but dependent on their protonation state. This high scavenging capacity is attributed to the deprotonated catechol group. In addition, both BPs showed a high chelation affinity for Cu(II) ions, suggesting a secondary antioxidant activity (inhibition of free radical production through metal sequestration). This study sheds light on the antioxidant mechanisms of marine BPs and highlights the impact of the nature of the interphenolic bond (C–O–C or C–C) as well as the catechol group on their efficacy.

Received 25th April 2025
Accepted 23rd June 2025

DOI: 10.1039/d5ra02914g

rsc.li/rsc-advances

1. Introduction

Bromophenols (BPs) are brominated derivatives of phenol, characterized by hydroxyl groups and bromine atoms attached to a benzene ring. These compounds are mainly found in marine algae, particularly red and brown seaweed species. Their structural diversity, due to variations in the number and position of bromine atoms, gives rise to a wide range of biological activities.[1–4] BPs have received particular attention for their health benefits, including anti-diabetic and anti-cancer properties.[3] For example, BPs extracted from *Symphyocladia latiuscula* have been shown to inhibit key enzymes involved in carbohydrate metabolism, such as hydrolysis enzymes and protein tyrosine phosphatase, which play a key role in insulin signaling and glucose regulation.[5] In addition, a BP derivative from *Rhodomela confervoides* has demonstrated notable anti-angiogenic effects along with PTP1B-inhibiting activity.[6,7] This compound also exhibited anti-cancer activity against several cell lines while showing lower cytotoxicity toward human umbilical vein endothelial cells (HUVECs).[8]

Among their various bioactive properties, BPs are particularly recognized for their potent antioxidant activity, primarily attributed to their ability to scavenge free radicals. Fig. 1 presents the molecular structures of selected BPs with significant antiradical activity as reported in the literature. BPs **1** and **2**, isolated from *Symphyocladia latiuscula* and *Polysiphonia urceolata*, respectively, exhibit notable DPPH free radical scavenging activity, with median inhibitory concentrations (IC_{50}) of 8.5 μM and 20.3 μM.[9,10] BPs **3** and **6**, also isolated from *Polysiphonia urceolata*, demonstrate strong *anti*-DPPH activity with IC_{50} values of 6.8 μM and 6.1 μM, respectively.[10] Nitrogen-containing BPs **4** and **5**, obtained from the red alga *Rhodomela confervoides*, exhibit potent DPPH radical scavenging activity (IC_{50} = 5.7 μM and 5.2 μM, respectively), markedly stronger than that of BHT (IC_{50} = 82.1 μM). However, their activity in the ABTS assay was relatively moderate, with TEAC values of 2.1 mM and 2.8 mM, respectively, compared to 1.0 mM for ascorbic acid.[11] Furthermore, compound **7**, derived from *Vertebrata lanosa*, outperforms reference antioxidants such as luteolin and quercetin in both the cellular antioxidant activity (CAA) and cellular lipid peroxidation antioxidant activity (CLPAA) assays.[12] Finally, (R)-rhodomelain A (**8**), isolated from *Rhodomela confervoides*, demonstrates outstanding antioxidant capacity, with IC_{50} values of 3.82 μM in the DPPH assay and 4.37 mM in the TEAC assay.[13] Although these studies collectively demonstrate the impressive antiradical capabilities of BPs, significant gaps in

Laboratory of Synthesis of Molecules with Biological Interest, Department of Chemistry, Faculty of Exact Sciences, University of Frères Mentouri Constantine 1, Constantine 25017, Algeria. E-mail: boulebd.houssem@umc.edu.dz

† Electronic supplementary information (ESI) available. See DOI: https://doi.org/10.1039/d5ra02914g

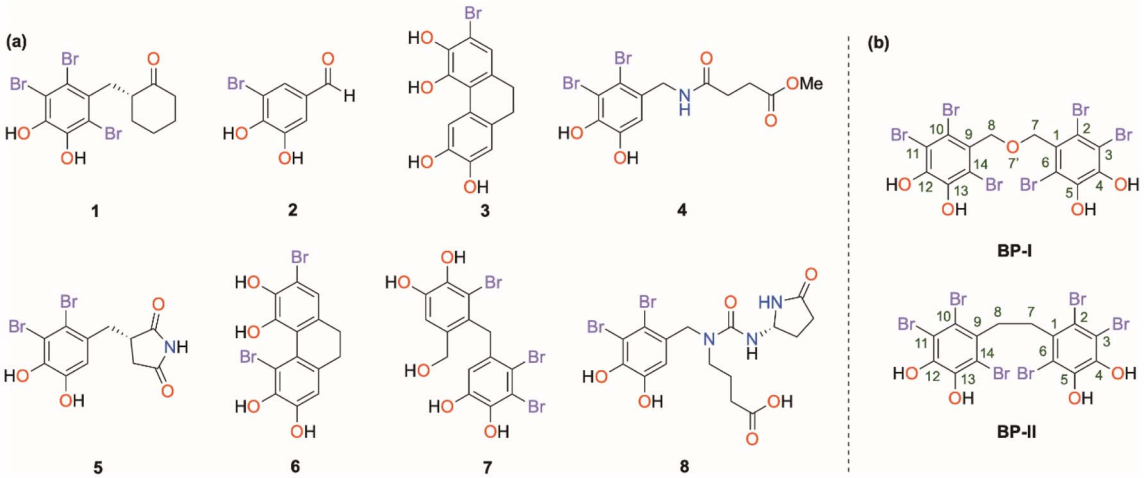

Fig. 1 (a) Naturally occurring bromophenol derivatives with potent antioxidant activity reported in the literature; (b) molecular structures of the bromophenols investigated in the current study.

knowledge remain. Current research has been mainly limited to *in vitro* tests, with surprisingly little *in vivo* validation of these antioxidant effects. In addition, we still lack clear data on structure–activity relationships that could help explain why certain BP structures exhibit greater activity than others. These unanswered questions underline the need for further exploration of the free radical scavenging properties of BPs.

The aim of this study is to investigate the radical scavenging capacity of two natural BP derivatives using computational approaches. The selected compounds, **BP-I** (5,5'-(oxybis(methylene))bis(3,4,6-tribromobenzene-1,2-diol)) and **BP-II** (5,5'-(ethane-1,2-diyl)bis(3,4,6-tribromobenzene-1,2-diol)) (Fig. 1), were analyzed to systematically explore their structure–activity relationship and assess how structural features influence antioxidant mechanisms. These BPs, naturally occurring in red algae *Symphyocladia latiuscula*, exhibit remarkable antioxidant properties, significantly surpassing the standard BHT in DPPH assay.[14] Beyond their radical-scavenging activity, these compounds show promising therapeutic potential. **BP-I** demonstrates potent protective effects against oxidative damage in HaCaT cells *via* Nrf2-mediated pathways.[15] It also functions as a moderately selective inhibitor of human monoamine oxidase-A (MAO-A) and displays significant agonist activity at dopamine D3/D4 receptors.[16] Notably, **BP-I** exhibits anti-diabetic properties through dual mechanisms: down-regulation of tyrosine phosphatase 1B (PTP1B) and α-glucosidase inhibition.[17] In addition, **BP-I** strongly antagonizes cholecystokinin 2 (CCK2) receptors, suggesting its potential in treating anxiety and depression disorders.[18] Meanwhile, **BP-II** displays remarkable anti-diabetic activity, inhibiting PTP1B with an IC_{50} value lower than that of the positive control sodium orthovanadate.[5] Structurally, both **BP-I** and **BP-II** contain catechol moieties and three bromine atoms, but they differ in their interunit linkages: **BP-I** features a flexible ether bridge (C–O–C), while **BP-II** possesses a rigid carbon–carbon bond (C–C).

The density functional theory (DFT) approach at the M06-2X/6-311++G(d,p) theoretical level was employed to investigate the antiradical mechanisms of **BP-I** and **BP-II**. This computational method has been previously validated for accurately modeling radical reactions.[19] The reactivity was assessed against hydroperoxyl radicals ($HOO^{\bullet}$), widely regarded as a reliable standard for evaluating antioxidant activity.[20] Several environmental and structural factors were considered, including medium polarity and the influence of OH group dissociation. The primary radical scavenging pathways, such as hydrogen atom transfer (HAT) and single-electron transfer (SET), were systematically examined. In addition, the complexation capacity of **BP-I** and **BP-II** toward Cu(II) ions was examined in physiological media to assess their potential secondary antioxidant activity. This evaluation provides further insights into the metal-chelating properties of these compounds and their role in mitigating oxidative stress through alternative antioxidant pathways.

2. Computation procedures

All density functional theory (DFT) calculations were conducted using the Gaussian 09 software package.[21] The hybrid meta exchange-correlation functional M06-2X, in combination with the 6-311++G(d,p) basis set, was employed to ensure high accuracy in thermodynamic and kinetic computations.[19,22,23] To account for solvation effects, Truhlar's SMD implicit solvation model was employed using the default parameters in Gaussian 09. Water and pentyl ethanoate were used to simulate aqueous and lipid environments, respectively.[24] Transition states (TSs) and ground states were characterized by imaginary frequency (IF) analysis, with the validation of TSs performed *via* intrinsic reaction coordinate (IRC) calculations. The frontier molecular orbitals (FMOs) were obtained using Multiwfn 3.8 software and visualized through VMD.[25,26] The pK_a values were calculated according to a protocol described in the literature.[27] The proton affinities (PAs) were calculated using the following equation:

$$PA = H(BP^{-}) + H(H^{+}) - H(BP - H) \quad (1)$$

where $H(BP^{-})$, $H(H^{+})$, and H(BP – H) are the enthalpies of the deprotonated BP, the proton, and the neutral BP, respectively.

Kinetic analyses were carried out using the quantum mechanics-based test for overall free radical scavenging activity (QM-ORSA).[28,29] The rate constants (k) were calculated *via* conventional transition state theory (TST), assuming a 1 M reference state at 298.15 K, using the expression:[30–32]

$$k = \sigma\kappa \frac{k_B T}{h} e^{-(\Delta G^{\neq})/RT} \quad (2)$$

where, σ is the reaction symmetry number,[33,34] κ denotes tunneling corrections calculated using the Eckart barrier,[35] k_B is the Boltzmann constant, h is the Planck constant, and $\Delta G^{\neq}$ represents the Gibbs free energy of activation.

The apparent rate constants (k_{app}) were adjusted considering the diffusion-limited regime *via* the Collins–Kimball model.[36] Branching ratios (Γ, %) for competing pathways were determined using:

$$\Gamma_{path} = \frac{k}{k_{overall}} \times 100 \quad (3)$$

where k corresponds to the rate constant of a specific pathway and $k_{overall}$ is the sum of all pathway rate constants.

To estimate the Gibbs free energy of activation for the single electron transfer mechanism, Marcus theory was applied:[37]

$$\Delta G^{\neq}_{SET} = \frac{\lambda}{4}\left(1 + \frac{\Delta G^{0}_{SET}}{\lambda}\right)^2 \quad (4)$$

$$\lambda \approx \Delta E_{SET} + \Delta G^{0}_{SET} \quad (5)$$

where, λ represents the nuclear reorganization energy, $\Delta G_{SET}{}^{0}$ is the Gibbs free energy of reaction, and ΔE_{SET} is the nonadiabatic energy difference between reactants and vertical products.

The sequestration of Cu(II) ions by **BP-I** and **BP-II** was investigated based on their chelating sites. The Gibbs free energy of complexation (ΔG°_{f}) was determined using the equilibrium reaction:

$$[Cu(H_2O)_4]^{2+} + BP^{n} \rightleftarrows [Cu(H_2O)_2BP]^{2+n} + 2H_2O \quad (6)$$

where n is the charge of the antioxidant and "BP" is **BP-I** or **BP-II**.

The apparent equilibrium constants (k_f) were then determined using the following equation:

$$k_f = e^{-\frac{\Delta G^{\circ}_{f}}{RT}} \quad (7)$$

3. Results and discussion

The radical scavenging activity of a phenolic compound occurs through three main pathways: (i) hydrogen atom transfer (HAT), (ii) single electron transfer (SET), and (iii) radical adduct formation (RAF). Hydrogen transfer can occur in two ways: (i) as a single-step transfer of an entire hydrogen atom between the same donor/acceptor sites, characteristic of the HAT mechanism, or (ii) through a transfer of an electron and a proton in a single elementary step but between different donor and acceptor sites, corresponding to the proton-coupled electron transfer (PCET) mechanism.[38] Despite their mechanistic differences, both pathways lead to the same final product and generally follow similar kinetics. Therefore, instead of focusing on their specific mechanistic details, we considered the overall process as formal hydrogen transfer (*f*-HAT). For single electron transfer (SET), this process can proceed *via* two possible pathways: (i) single electron transfer–proton transfer (SETPT) where the electron transfer occurs from the neutral molecule, or (ii) single proton transfer–electron transfer (SPTET) where the electron transfer occurs from the deprotonated compound. Both pathways were considered in our study. Regarding radical adduct formation (RAF), this mechanism is generally unfavorable for the hydroperoxyl radical when a phenolic antioxidant is involved.[39,40] Consequently, it was not included in our study.

3.1 Molecular geometry and frontier molecular orbitals

Since molecular geometry plays a crucial role in the antioxidant activity of phenolic compounds, the structures of **BP-I** and **BP-II** were first determined in the gas phase by performing

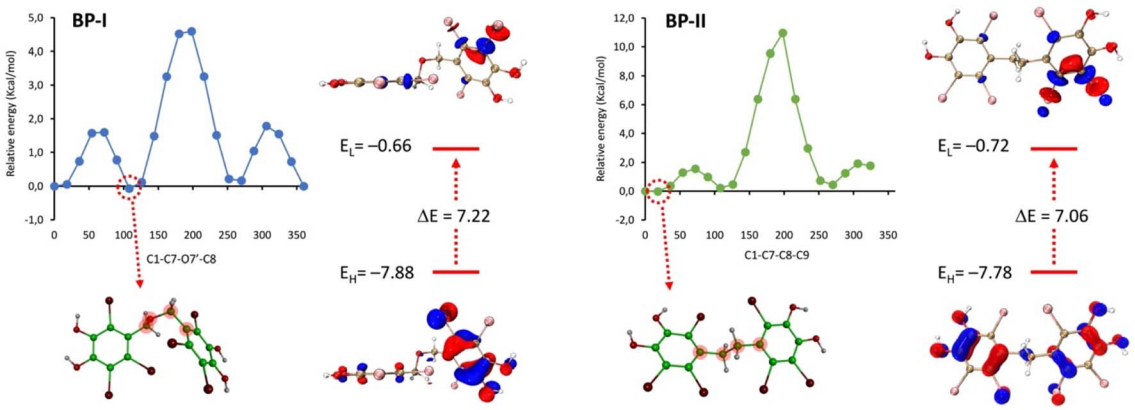

Fig. 2 Relaxed potential energy scans of the dihedral angles C1–C7–O7′–C8 (**BP-I**) and C1–C7–C8–C9 (**BP-II**), performed in the gas phase at the M06-2X/6-311++G(d,p) level of theory. At each step, the dihedral angle was varied while all other geometrical parameters were optimized. The computed distributions and energies of the frontier molecular orbitals (FMOs) of the most stable geometry of both compounds are also shown.

a rotational scan study. This study focused on the potential rotation of the phenolic groups through the C–O–C or C–C linkages. A total of twenty steps, each with an interval of 18°, were examined, as illustrated in Fig. 2.

The analysis of the results revealed that the two compounds adopt different geometrical arrangements: **BP-I** assumes an inclined geometry, whereas **BP-II** adopts a relatively linear conformation. Based on these optimized geometries, the frontier molecular orbitals (FMOs) of both compounds were computed, and the results are presented in Fig. 2. As observed, the highest occupied molecular orbital (HOMO) in both **BP-I** and **BP-II** is delocalized throughout the entire molecule, suggesting that the whole structure may participate in nucleophilic attacks. In contrast, the lowest unoccupied molecular orbitals (LUMOs) are primarily localized on the adjacent bromine atoms, indicating that these sites may be the most reactive for electrophilic attacks.

Regarding the energy levels, the HOMO energy (E_{HOMO}) of **BP-II** is slightly higher than that of **BP-I** (−7.78 *vs.* −7.88 eV), suggesting that **BP-II** may exhibit greater electron-donating

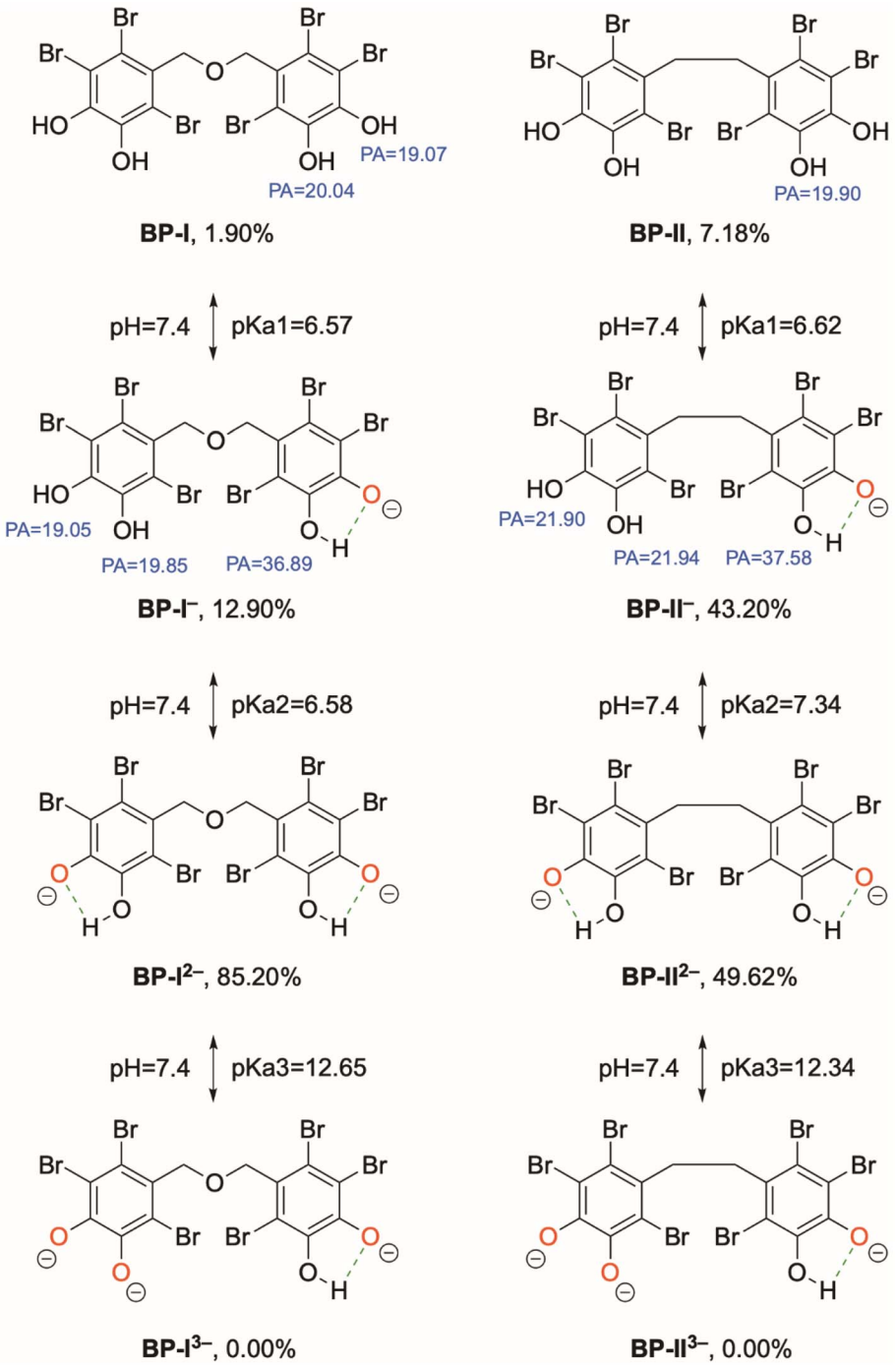

Fig. 3 Calculated proton affinities (PA, in kcal mol^{-1}), pK_a values, and acid–base equilibrium at pH = 7.4 of BP-I and BP-II.

Table 1 Kinetic data of the reactions of HOO˙ radicals with **BP-I** and **BP-II** in pentyl ethanoate

Compound	Position	ΔG (kcal mol^{-1} R^{-1})	IF[a] (cm^{-1})	$\Delta G^{\neq}$[b] (kcal mol^{-1})	κ[c]	k[d] (M^{-1} s^{-1})	Γ[e] (%)	$k_{overall}$ (M^{-1}s^{-1})
BP-I	4OH	−3.3	−2224.8	17.6	150.5	1.20×10^2	50	2.40×10^2
	5OH	−3.7	−2187.2	17.4	115.9	1.20×10^2	50	
BP-II	4OH	−3.8	−2167.9	16.4	103.8	6.60×10^2	38	1.76×10^3
	5OH	−4.0	−2159.4	15.9	88.9	1.10×10^3	62	

[a] maginary frequency. [b] Activation free energy. [c] Tunneling correction. [d] Rate constant, and. [e] Branching ratio.

ability and thus higher reactivity. On the other hand, the HOMO–LUMO energy gap of **BP-II** is lower than that of **BP-I** (−7.06 *vs.* −7.22 eV), implying that **BP-II** may be more chemically reactive than **BP-I**.

3.2 Acid-base equilibrium in water

Acid-base equilibrium in aqueous media influences the reactivity of phenolic compounds, in particular their ability to interact with free radicals.[41,42] Consequently, the deprotonation of the OH groups of the two BPs (**BP-I** and **BP-II**) at physiological pH (7.4) was examined by calculating their proton affinities (PA) and acidity constants (pK_a) (Fig. 3). The results reveal a multi-step deprotonation process. The first deprotonation occurs on the OH in position 4 of both BPs, with pK_a values of 6.57 for **BP-I** and 6.62 for **BP-II**. A second deprotonation subsequently takes place on the other OH in position 12, leading to doubly deprotonated species characterized by pK_a values of 6.58 (**BP-I**) and 7.34 (**BP-II**). A third deprotonation, although possible on the OH in position 13, is much less favorable, as evidenced by the high pK_a values of 12.65 (**BP-I**) and 12.34 (**BP-II**). The relatively low pK_a values of the singly and doubly deprotonated species can be attributed to the presence of an intramolecular hydrogen bond between the deprotonated oxygen and the adjacent hydroxyl group (Fig. 3). This interaction effectively stabilizes the negative charge, thereby facilitating deprotonation.

At physiological pH, the BPs exist in three main forms in equilibrium. The neutral form is poorly present, with only 1.90% for **BP-I** and 7.18% for **BP-II**. The mono-deprotonated form is asymmetrically distributed, being dominant in **BP-II** (43.20%) but minor in **BP-I** (12.90%). On the other hand, the doubly deprotonated form clearly dominates for **BP-I** (85.20%), while being significantly present for **BP-II** (49.62%). The triple-deprotonated form, in contrast, is thermodynamically inaccessible under these conditions. These different species, whose relative proportions vary significantly between **BP-I** and **BP-II**, were all considered in the following thermodynamic and kinetic studies.

3.3 HOO˙ scavenging under physiological media

The HOO˙ scavenging activity of **BP-I** and **BP-II** was evaluated following the QM-ORSA protocol in both polar and lipid media. In lipid environments, the BPs exist exclusively in their neutral form and can react only *via* the *f*-HAT mechanism. In contrast, in aqueous media, several dissociated forms of BPs may coexist, allowing reactions to proceed *via* both *f*-HAT and SET mechanisms. All possible reaction pathways at potentially reactive sites were considered, and the outcomes are presented in

Table 2 Kinetic data of the reactions of HOO˙ radicals with **BP-I** and **BP-II** in water

Comp.	Mechanism		State	ΔG (Kcal mol^{-1})	$\Delta G^{\neq}$ (Kcal mol^{-1})	κ	k_{app} (M^{-1} s^{-1})	f[a]	k_f[b] (M^{-1} s^{-1})	Γ (%)	$k_{overall}$ (M^{-1} s^{-1})
BP-I	*f*-HAT	4OH	H3A	−4.59	17.84	405.87	2.10×10^2	0.019	3.99×10^0	0	1.96×10^9
		5OH		−5.21	18.26	336.47	8.56×10^1		1.63×10^0	0	
	f-HAT	5OH	H2A	−13.3	—	—	2.00×10^9 [d]	0.129	2.58×10^8	13	
		4′OH		3.04	17.19	39.63	6.11×10^1		7.88×10^0	0	
		5′OH		−6.45	17.16	261.30	4.28×10^2		5.52×10^1	0	
	SET			10.98	11.52	17.04[c]	2.23×10^4		2.28×10^3	0	
	f-HAT	5OH	HA	−13.5	—	—	2.00×10^9 [d]	0.852	1.70×10^9	87	
	SET			18.57	18.83	14.68[c]	9.77×10^{-2}		8.32×10^{-2}	0	
BP-II	*f*-HAT	4OH	H3A	−5.98	19.15	1530.34	8.64×10^1	0.072	6.22×10^0	0	2.04×10^9
		5OH		−6.52	19.20	1598.88	8.36×10^1		6.22×10^0	0	
	f-HAT	5OH	H2A	−13.9	—	—	2.20×10^9 [d]	0.432	9.50×10^8	47	
		4′OH		1.97	19.02	421.40	2.98×10^1		1.29×10^1	0	
		5′OH		−5.96	19.09	1542.87	9.73×10^1		4.20×10^1	0	
	SET			9.41	10.15	16.40[c]	2.23×10^5		9.63×10^4	0	
	f-HAT	5OH	HA	−14.6	—	—	2.20×10^9 [d]	0.496	1.09×10^9	53	
	SET			15.1	15.10	15.18[c]	5.29×10^1		2.62×10^1	0	

[a] Mole fraction. [b] $k_f = f.k_{app}$. [c] The nuclear reorganization energy (λ). [d] Diffusion rate constant.

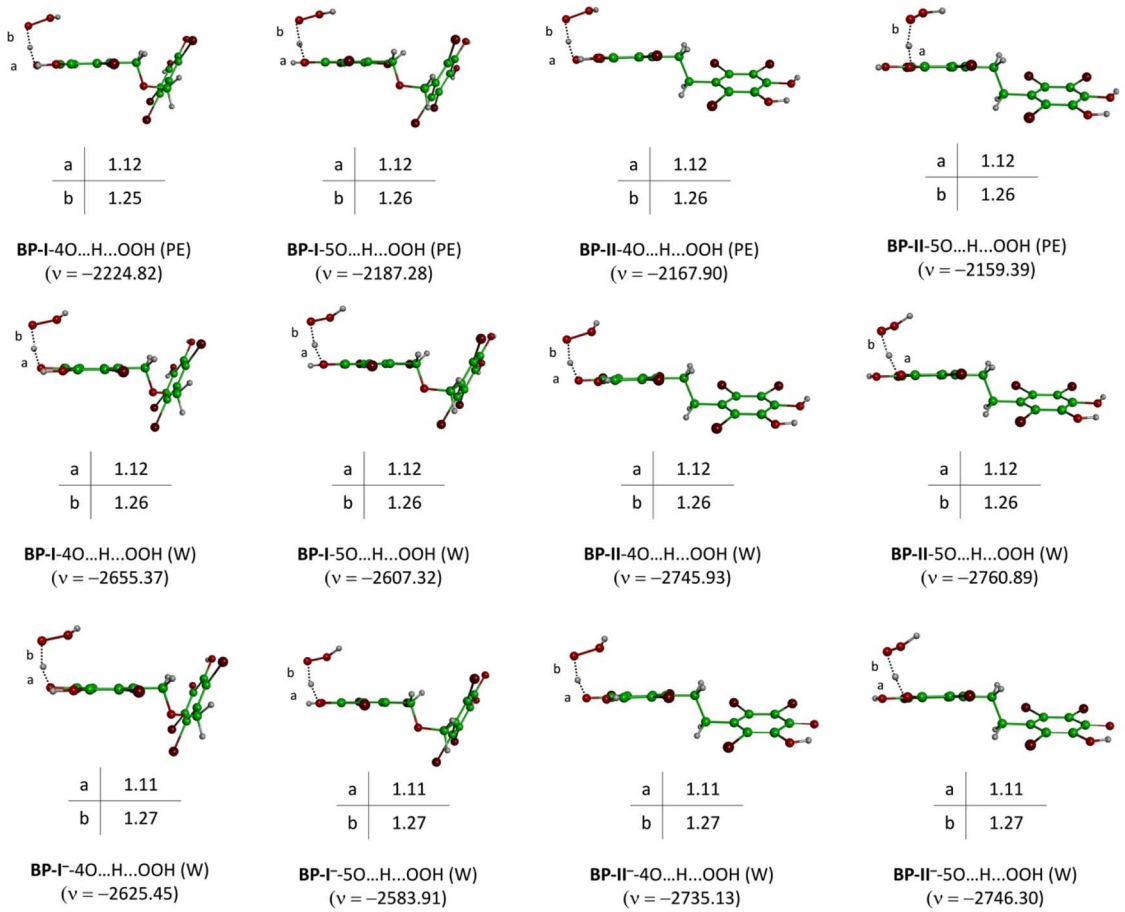

Fig. 4 Localized TSs of the reactions between BP-I/BP-II and HOO˙ radical following the *f*-HAT mechanism in pentylethanoate (PE) and water (W). Imaginary frequencies (ν) are in cm^{-1} and distances are in Å.

Tables 1 and 2. The localized transition states of the *f*-HAT pathways are illustrated in Fig. 4.

As shown in Table 1, the reaction between both BPs and HOO˙ is spontaneous at all OH groups, with ΔG values ranging from −3.3 to −4.0 kcal mol^{-1}. The overall rate constant ($k_{overall}$) for **BP-I** is 2.40×10^2 M^{-1} s^{-1}, while that of **BP-II** is 1.76×10^3 M^{-1} s^{-1}, indicating that **BP-II** is approximately seven times more active than **BP-I.** This result suggests that the C–C linkage is more favorable for antiradical activity than the C–O–C linkage in pentyl ethanoate. Regarding attack sites, the reaction tends to take place on both 5-OH and 4-OH groups for both BPs.

The rate constants of **BP-I** and **BP-II** are somewhat comparable to or slightly lower than those of common antioxidants, such as Trolox ($k = 3.40 \times 10^3$ M^{-1} s^{-1}),[43] and BHT ($k_{overall} = 1.70 \times 10^4$ M^{-1} s^{-1}).[44] This indicates that BPs—particularly **BP-II**—are effective HOO˙ scavengers in lipid media.

In aqueous media, as shown in Table 2, the *f*-HAT mechanism was predominantly spontaneous across most investigated positions, with ΔG values ranging from −4.59 to −14.6 kcal mol^{-1}. However, at the 4′-OH position in the mono-deprotonated form, the reaction was exergonic, with ΔG values of 3.04 and 1.97 kcal mol^{-1} for **BP-I** and **BP-II**, respectively. The lowest ΔG values were observed at the deprotonated catechol groups (both mono- and doubly deprotonated forms), ranging from −13.3 to −14.6 kcal mol^{-1}. In contrast, all SET processes were endergonic for both compounds, with ΔG values between 9.41 and 18.57 kcal mol^{-1}.

The overall rate constants of **BP-I** and **BP-II** were comparable, with values of 1.96×10^9 and 2.04×10^9 M^{-1} s^{-1}, respectively. The *f*-HAT mechanism from the deprotonated catechol group was identified as the dominant reaction pathway for both BPs, contributing entirely to the overall rate constants. This pronounced reactivity of the catechol moiety aligns with previous studies on natural antioxidants such as caffeoyl tryptamine ($k_{overall} = 3.15 \times 10^8$ M^{-1} s^{-1}),[45] quercetin ($k_{overall} = 8.11 \times 10^9$ M^{-1} s^{-1}),[46] anthocyanidins ($k_{overall} \sim 10^9$ M^{-1} s^{-1})[47] and caftaric acid ($k_{overall} = 9.09 \times 10^8$ M^{-1} s^{-1}).[48] Compared to the common antioxidants Trolox ($k_{overall} = 8.96 \times 10^4$ M^{-1} s^{-1})[43] and BHT ($k_{overall} = 2.51 \times 10^5$ M^{-1} s^{-1}),[44] **BP-I** and **BP-II** exhibit significantly higher reactivity, positioning them as potent antioxidants in polar media.

Analysis of the results in Table 2 suggests that in their neutral forms, both BPs function as moderate radical scavengers (rate constants within the range of 8.56×10^1 to 2.10×10^2 $M^{-1}s^{-1}$). Their exceptional reactivity is primarily attributed to their deprotonated state, indicating that under neutral and basic conditions, BPs act as highly effective radical scavengers.

However, their efficiency declines significantly in acidic environments.

Overall, the findings from both polar and lipid media suggest that **BP-I** and **BP-II** perform well as radical scavengers in lipid environments but exhibit outstanding scavenging potential in polar media at physiological pH.

3.4 Metal chelating capacity in water

Another critical aspect of the antioxidant activity of phenolic compounds is their ability to chelate transition metal ions. These ions, such as copper (Cu), play a significant role in oxidative stress by catalyzing the formation of highly reactive hydroxyl radicals (HO$^{\bullet}$) *via* the Fenton reaction.[49,50] In this process, Cu(I) reacts with hydrogen peroxide (H_2O_2), generating Cu(II), a hydroxyl radical, and a hydroxide ion:

$$Cu^{+} + H_2O_2 \rightarrow Cu^{2+} + HO^{\bullet} + HO^{-} \quad (8)$$

Under physiological conditions, however, Cu(I) is not the most stable or predominant form of copper. The redox equilibrium between Cu(I) and Cu(II) is maintained through

Table 3 Computed Gibbs free energy of formation (ΔG_f in kcal mol^{-1}) and kinetic rate constants (k, k_f, and $k_{overall}$ in M^{-1} s^{-1}) of the potential complexation reactions of BP-I and BP-II with Cu(II) ions in water

Reaction	ΔG_f	k	f	k_f	Γ	$k_{overall}$
$Cu(H_2O)_4^{2+}$ + **BP-I** → $[Cu(H_2O)_2$**BP-I**$]^{2+}$	7.12	9.49×10^{-6}	0.019	1.23×10^{-7}	0	3.96×10^{9}
$Cu(H_2O)_4^{2+}$ + **BP-I**$^{-}$ → $[Cu(H_2O)_2$**BP-I**$]^{+}$	−12.72	1.84×10^{9}	0.129	2.38×10^{8}	6	
$Cu(H_2O)_4^{2+}$ + **BP-I**$^{2-}$ → $Cu(H_2O)_2$**BP-I**	−13.24	4.36×10^{9}	0.852	3.72×10^{9}	94	
$Cu(H_2O)_4^{2+}$ + **BP-II** → $[Cu(H_2O)_2$**BP-II**$]^{2+}$	5.83	5.66×10^{-5}	0.072	4.08×10^{-6}	0	3.86×10^{10}
$Cu(H_2O)_4^{2+}$ + **BP-II**$^{2-}$ → $[Cu(H_2O)_2$**BP-II**$]^{+}$	−14.40	3.04×10^{10}	0.432	1.31×10^{10}	34	
$Cu(H_2O)_4^{2+}$ + **BP-II**$^{2-}$ → $Cu(H_2O)_2$**BP-II**	−14.71	5.13×10^{10}	0.496	2.54×10^{10}	66	

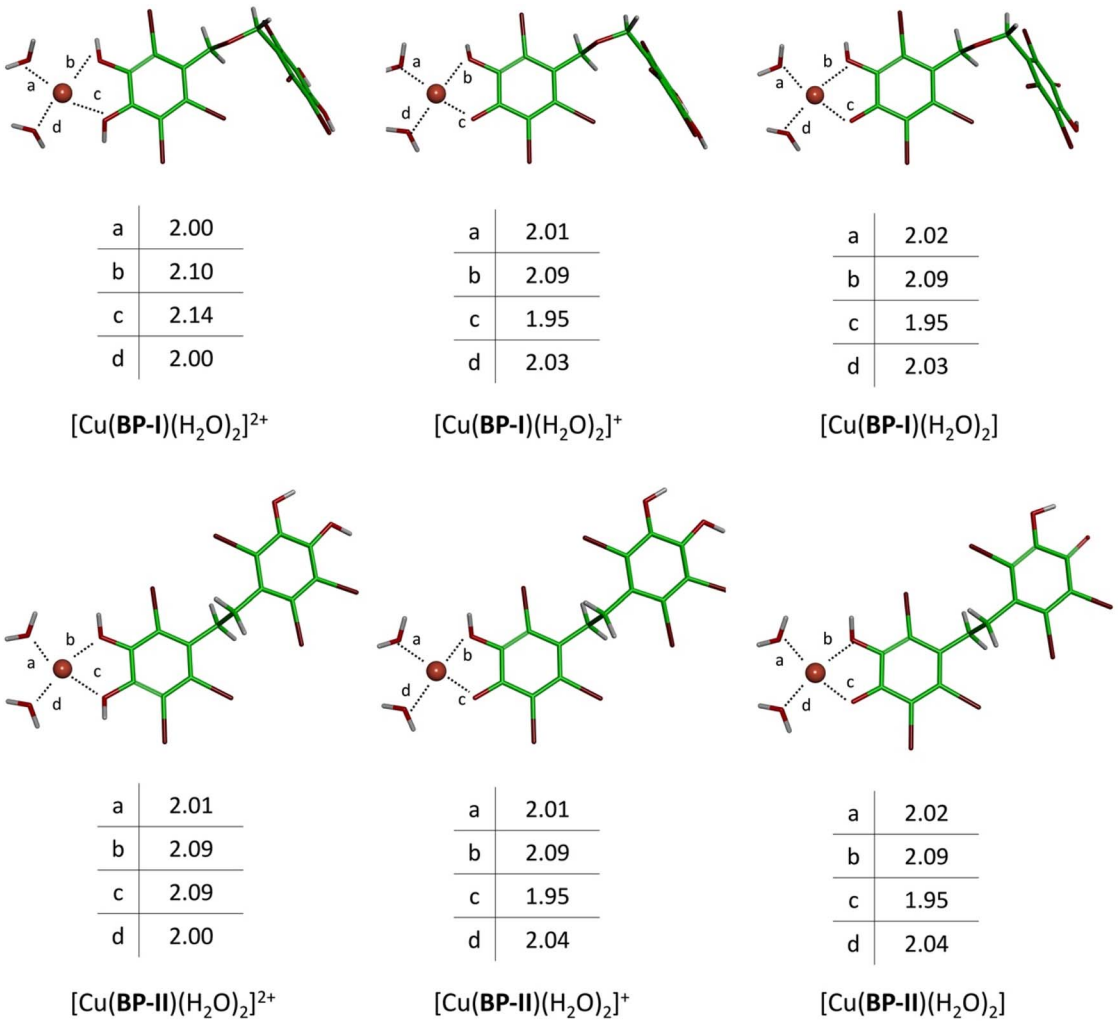

Fig. 5 Optimized molecular structure of potential Cu(II)- BPs complexes in water. Distances are in Å.

reduction reactions involving endogenous reductants like the ascorbate anion (Asc^-) or the superoxide radical ($O_2^{\bullet -}$), as described in the following equations:

$$Cu^{2+} + O_2^{\bullet -} \rightarrow Cu^+ + O_2 \quad (9)$$

$$Cu^{2+} + Asc^- \rightarrow Cu^+ + Asc^{\bullet} \quad (10)$$

The concentration of Cu(I) at equilibrium is therefore governed by the efficiency of these reduction processes. Phenolic compounds with metal-chelating properties can disrupt this equilibrium by binding to Cu(II), forming stable complexes that prevent its reduction to Cu(I). By sequestering Cu(II), these antioxidants disrupt the catalytic cycle of hydroxyl radical generation, providing an indirect but effective mechanism for mitigating oxidative damage.

The Cu(II) chelation capacity of **BP-I** and **BP-II** was systematically studied in aqueous medium at pH = 7.4. The potential complexation reactions are shown in Table 3 and the optimized structures of the complexes are shown in Fig. 5. Both compounds demonstrated a higher affinity for Cu(II) ions in their dissociated forms than in their neutral states, forming stable complexes with Gibbs free energies of formation (ΔG_f) ranging from −12.72 to −14.71 kcal mol^{-1}. Under the conditions studied, the dissociated forms' complexes account for 100% of the possible complexes.

Further analysis of the reaction equilibrium constants, derived from Maxwell–Boltzmann calculations, revealed exceptionally high binding kinetics. **BP-I** and **BP-II** exhibited rate constants of 3.96×10^9 M^{-1} s^{-1} and 3.86×10^{10} M^{-1} s^{-1}, respectively, confirming their efficacy as Cu(II) chelators. These results suggest that, in addition to their established radical-scavenging activity (primary antioxidant), **BP-I** and **BP-II** can also function as secondary antioxidants, effectively attenuating metal-induced oxidative stress by sequestering Cu(II) ions and disrupting redox cycle pathways.

4. Conclusion

The radical scavenging capacity and metal chelation potential of two natural BP derivatives found in marine algae have been systematically investigated using DFT calculations. The studied BPs were identified as effective HOO$^{\bullet}$ scavengers in lipid media, acting exclusively *via* the *f*-HAT mechanism at both the 4-OH and 5-OH positions. Under these conditions, **BP-I**, which contains a C–C linkage, was found to be more reactive than **BP-II**, which features a C–O–C linkage, highlighting the influence of the linkage type in lipid environments. In contrast, both BPs exhibited excellent HOO$^{\bullet}$ scavenging activity in water, with comparable rate constants in the order of 10^9 M^{-1} s^{-1}. This high reactivity is attributed to the deprotonated catechol group, which serves as the primary driving force behind their radical scavenging activity. The acid–base equilibrium also plays a crucial role in the radical scavenging efficiency of BPs. While their reactivity is moderate under acidic conditions, it increases significantly in neutral and basic environments. Additionally, **BP-I** and **BP-II** demonstrated a strong capacity for Cu(II) ion chelation, suggesting the potential for secondary antioxidant activity. In light of these findings, **BP-I** and **BP-II** could be considered potent natural antioxidants, particularly in polar media. This study provides valuable insights that could guide the design of new, highly effective antioxidants for pharmacological and food applications.

Data availability

The data supporting this article have been included as part of the ESI.†

Conflicts of interest

The author has no conflicts of interest to declare.

Acknowledgements

The supercomputing resources used in this work were supported by the HPC of UCI-UFMC (Unité de Calcul Intesif of the University Fréres Mentouri Constantine 1).

References

1 P. Barciela, M. Carpena, A. Perez-Vazquez, A. Silva, A. O. S. Jorge and M. A. Prieto, Bromophenols in Red Algae: Exploring the Chemistry and Uncovering Biological Benefits of These Unknown Compounds, *Biol. Life Sci. Forum*, 2024, **35**(1), 11, DOI: 10.3390/blsf2024035011.

2 M. Liu, P. E. Hansen and X. Lin, Bromophenols in Marine Algae and Their Bioactivities, *Mar. Drugs*, 2011, 1273–1292.

3 A. A. El Gamal, Biological importance of marine algae, *Saudi Pharm. J.*, 2010, **18**(1), 1–25, DOI: 10.1016/j.jsps.2009.12.001.

4 V. K. Mandrekar, U. B. Gawas and M. S. Majik, Chapter 13 - Brominated Molecules From Marine Algae and Their Pharmacological Importance, in *Studies in Natural Products Chemistry*, ed. R. Atta ur, Elsevier, 2019, pp. , pp. 461–490.

5 X. Liu, X. Li, L. Gao, C. Cui, C. Li, J. Li and B. Wang, Extraction and PTP1B inhibitory activity of bromophenols from the marine red alga Symphyocladia latiuscula, *Chin. J. Oceanol. Limnol.*, 2011, **29**(3), 686–690, DOI: 10.1007/s00343-011-0136-1.

6 S. Wang, L.-J. Wang, B. Jiang, N. Wu, X. Li, S. Liu, J. Luo and D. Shi, Anti-Angiogenic Properties of BDDPM, a Bromophenol from Marine Red Alga Rhodomela confervoides, with Multi Receptor Tyrosine Kinase Inhibition Effects, *Int. J. Mol. Sci.*, 2015, 13548–13560.

7 J. Li, S. J. Guo, H. Su, L. J. Han and D. Y. Shi, Total synthesis of bis-(2,3-dibromo-4,5-dihydroxyphenyl)-methane as potent PTP1B inhibitor, *Chin. Chem. Lett.*, 2008, **19**(11), 1290–1292, DOI: 10.1016/j.cclet.2008.07.002.

8 N. Wu, J. Luo, B. Jiang, L. Wang, S. Wang, C. Wang, C. Fu, J. Li and D. Shi, Marine Bromophenol Bis (2,3-Dibromo-4,5-dihydroxy-phenyl)-methane Inhibits the Proliferation, Migration, and Invasion of Hepatocellular Carcinoma Cells *via* Modulating ?1-Integrin/FAK Signaling, *Mar. Drugs*, 2015, 1010–1025.

9 J. S. Choi, H. J. Park, H. A. Jung, H. Y. Chung, J. H. Jung and W. C. Choi, A Cyclohexanonyl Bromophenol from the Red Alga Symphyocladia latiuscula, *J. Nat. Prod.*, 2000, **63**(12), 1705–1706, DOI: 10.1021/np0002278.

10 K. Li, X.-M. Li, N.-Y. Ji and B.-G. Wang, Bromophenols from the Marine Red Alga Polysiphonia urceolata with DPPH Radical Scavenging Activity, *J. Nat. Prod.*, 2008, **71**(1), 28–30, DOI: 10.1021/np070281p.

11 K. Li, X.-M. Li, J. B. Gloer and B.-G. Wang, New nitrogen-containing bromophenols from the marine red alga Rhodomela confervoides and their radical scavenging activity, *Food Chem.*, 2012, **135**(3), 868–872, DOI: 10.1016/j.foodchem.2012.05.117.

12 E. K. Olsen, E. Hansen, J. Isaksson and J. H. Andersen, Cellular Antioxidant Effect of Four Bromophenols from the Red Algae, Vertebrata lanosa, *Mar. Drugs*, 2013, 2769–2784.

13 K. Li, Y.-F. Wang, X.-M. Li, W.-J. Wang, X.-Z. Ai, X. Li, S.-Q. Yang, J. B. Gloer, B.-G. Wang and T. Xu, Isolation, Synthesis, and Radical-Scavenging Activity of Rhodomelin A, a Ureidobromophenol from the Marine Red Alga Rhodomela confervoides, *Org. Lett.*, 2018, **20**(2), 417–420, DOI: 10.1021/acs.orglett.7b03716.

14 X.-J. Duan, X.-M. Li and B.-G. Wang, Highly Brominated Mono- and Bis-phenols from the Marine Red Alga Symphyocladia latiuscula with Radical-Scavenging Activity, *J. Nat. Prod.*, 2007, **70**(7), 1210–1213, DOI: 10.1021/np070061b.

15 H. Dong, M. Liu, L. Wang, Y. Liu, X. Lu, D. Stagos, X. Lin and M. Liu, Bromophenol Bis (2,3,6-Tribromo-4,5-dihydroxybenzyl) Ether Protects HaCaT Skin Cells from Oxidative Damage *via* Nrf2-Mediated Pathways, *Antioxidants*, 2021, **10**(9), DOI: 10.3390/antiox10091436.

16 P. Paudel, S. E. Park, S. H. Seong, H. A. Jung and J. S. Choi, Bromophenols from Symphyocladia latiuscula Target Human Monoamine Oxidase and Dopaminergic Receptors for the Management of Neurodegenerative Diseases, *J. Agric. Food Chem.*, 2020, **68**(8), 2426–2436, DOI: 10.1021/acs.jafc.0c00007.

17 P. Paudel, S. H. Seong, H. J. Park, H. A. Jung and J. S. Choi, Anti-Diabetic Activity of 2,3,6-Tribromo-4,5-Dihydroxybenzyl Derivatives from Symphyocladia latiuscula through PTP1B Downregulation and α-Glucosidase Inhibition, *Mar. Drugs*, 2019, **17**(3), 166, DOI: 10.3390/md17030166.

18 P. Paudel, S. E. Park, S. H. Seong, F. M. Fauzi, H. A. Jung and J. S. Choi, Bromophenols from Symphyocladia latiuscula (Harvey) Yamada as Novel Cholecystokinin 2 Receptor Antagonists, *JIN*, 2023, **22**(1), 10, DOI: 10.31083/j.jin2201010.

19 A. Galano and J. R. Alvarez-Idaboy, Kinetics of radical-molecule reactions in aqueous solution: a benchmark study of the performance of density functional methods, *J. Comput. Chem.*, 2014, **35**(28), 2019–2026, DOI: 10.1002/jcc.23715.

20 M. Spiegel, Current Trends in Computational Quantum Chemistry Studies on Antioxidant Radical Scavenging Activity, *J. Chem. Inf. Model.*, 2022, **62**(11), 2639–2658, DOI: 10.1021/acs.jcim.2c00104.

21 M. J. Frisch, G. W. Trucks, H. B. Schlegel, G. E. Scuseria, M. A. Robb, J. R. Cheeseman, G. Scalmani, V. Barone, B. Mennucci, G. A. Petersson, H. Nakatsuji, M. Caricato, X. Li, H. P. Hratchian, A. F. Izmaylov, J. Bloino, G. Zheng, J. L. Sonnenberg, M. Hada, M. Ehara, K. Toyota, R. Fukuda, J. Hasegawa, M. Ishida, T. Nakajima, Y. Honda, O. Kitao, H. Nakai, T. Vreven, J. A. Montgomery Jr, J. E. Peralta, F. Ogliaro, M. Bearpark, J. J. Heyd, E. Brothers, K. N. Kudin, V. N. Staroverov, R. Kobayashi, J. Normand, K. Raghavachari, A. Rendell, J. C. Burant, S. S. Iyengar, J. Tomasi, M. Cossi, N. Rega, J. M. Millam, M. Klene, J. E. Knox, J. B. Cross, V. Bakken, C. Adamo, J. Jaramillo, R. Gomperts, R. E. Stratmann, O. Yazyev, A. J. Austin, R. Cammi, C. Pomelli, J. W. Ochterski, R. L. Martin, K. Morokuma, V. G. Zakrzewski, G. A. Voth, P. Salvador, J. J. Dannenberg, S. Dapprich, A. D. Daniels, Ö. Farkas, J. B. Foresman, J. V. Ortiz, J. Cioslowski and D. J. Fox, *Gaussian* 09, Gaussian, Inc., Wallingford CT, 2009.

22 Y. Zhao and D. G. Truhlar, The M06 suite of density functionals for main group thermochemistry, thermochemical kinetics, noncovalent interactions, excited states, and transition elements: two new functionals and systematic testing of four M06-class functionals and 12 other functionals, *Theor. Chem. Acc.*, 2008, **120**(1), 215–241, DOI: 10.1007/s00214-007-0310-x.

23 Y. Zhao and D. G. Truhlar, How Well Can New-Generation Density Functionals Describe the Energetics of Bond-Dissociation Reactions Producing Radicals?, *J. Phys. Chem. A*, 2008, **112**(6), 1095–1099, DOI: 10.1021/jp7109127.

24 A. V. Marenich, C. J. Cramer and D. G. Truhlar, Universal Solvation Model Based on Solute Electron Density and on a Continuum Model of the Solvent Defined by the Bulk Dielectric Constant and Atomic Surface Tensions, *J. Phys. Chem. B*, 2009, **113**(18), 6378–6396, DOI: 10.1021/jp810292n.

25 T. Lu and F. Chen, Multiwfn: A multifunctional wavefunction analyzer, *J. Comput. Chem.*, 2012, **33**(5), 580–592, DOI: 10.1002/jcc.22885.

26 W. Humphrey, A. Dalke and K. Schulten, VMD: visual molecular dynamics, *J. Mol. Graphics*, 1996, **14**(1), 33–38, DOI: 10.1016/0263-7855(96)00018-5.

27 A. Galano, A. Pérez-González, R. Castañeda-Arriaga, L. Muñoz-Rugeles, G. Mendoza-Sarmiento, A. Romero-Silva, A. Ibarra-Escutia, A. M. Rebollar-Zepeda, J. R. León-Carmona, M. A. Hernández-Olivares and J. R. Alvarez-Idaboy, Empirically Fitted Parameters for Calculating pKa Values with Small Deviations from Experiments Using a Simple Computational Strategy, *J. Chem. Inf. Model.*, 2016, **56**(9), 1714–1724, DOI: 10.1021/acs.jcim.6b00310.

28 A. Galano and J. R. Alvarez-Idaboy, A computational methodology for accurate predictions of rate constants in solution: application to the assessment of primary antioxidant activity, *J. Comput. Chem.*, 2013, **34**(28), 2430–2445, DOI: 10.1002/jcc.23409.

29 A. Galano and J. R. Alvarez-Idaboy, Computational strategies for predicting free radical scavengers' protection against oxidative stress: Where are we and what might follow?, *Int.*

J. Quantum Chem., 2019, **119**(2), e25665, DOI: 10.1002/qua.25665.

30 M. G. Evans and M. Polanyi, Some applications of the transition state method to the calculation of reaction velocities, especially in solution, *Trans. Faraday Soc.*, 1935, 875–894, DOI: 10.1039/TF9353100875.

31 H. Eyring, The Activated Complex in Chemical Reactions, *J. Chem. Phys.*, 1935, **3**(2), 107–115, DOI: 10.1063/1.1749604.

32 D. G. Truhlar, W. L. Hase and J. T. Hynes, Current Status of Transition-State Theory, *J. Phys. Chem. A*, 1983, **87**(15), 2664–2682, DOI: 10.1021/jp953748q.

33 E. Pollak and P. Pechukas, Symmetry numbers, not statistical factors, should be used in absolute rate theory and in Broensted relations, *J. Am. Chem. Soc.*, 1978, **100**(10), 2984–2991, DOI: 10.1021/ja00478a009.

34 A. Fernández-Ramos, B. A. Ellingson, R. Meana-Pañeda, J. M. Marques and D. G. Truhlar, Symmetry numbers and chemical reaction rates, *Theor. Chem. Acc.*, 2007, **118**(4), 813–826, DOI: 10.1007/s00214-007-0328-0.

35 C. Eckart, The penetration of a potential barrier by electrons, *Phys. Rev.*, 1930, **35**(11), 1303, DOI: 10.1103/PhysRev.35.1303.

36 F. C. Collins and G. E. Kimball, Diffusion-controlled reaction rates, *J. Colloid Interface Sci.*, 1949, **4**(4), 425–437, DOI: 10.1016/0095-8522(49)90023-9.

37 J. C. Corchado, E. L. Coitino, Y.-Y. Chuang, P. L. Fast and D. G. Truhlar, Interpolated variational transition-state theory by mapping, *J. Phys. Chem. A*, 1998, **102**(14), 2424–2438, DOI: 10.1021/jp9801267.

38 J. J. Warren, T. A. Tronic and J. M. Mayer, Thermochemistry of Proton-Coupled Electron Transfer Reagents and its Implications, *Chem. Rev.*, 2010, **110**(12), 6961–7001, DOI: 10.1021/cr100085k.

39 H. Boulebd, Is cannabidiolic acid an overlooked natural antioxidant? Insights from quantum chemistry calculations, *New J. Chem.*, 2022, **46**(1), 162–168, DOI: 10.1039/D1NJ04771J.

40 H. Boulebd and M. Spiegel, Computational assessment of the primary and secondary antioxidant potential of alkylresorcinols in physiological media, *RSC Adv.*, 2023, **13**(42), 29463–29476, DOI: 10.1039/D3RA05967G.

41 H. Boulebd, M. Carmena-Bargueño and H. Pérez-Sánchez, Exploring the Antioxidant Properties of Caffeoylquinic and Feruloylquinic Acids: A Computational Study on Hydroperoxyl Radical Scavenging and Xanthine Oxidase Inhibition, *Antioxidants*, 2023, **12**(9), 1669, DOI: 10.3390/antiox12091669.

42 H. Boulebd, Insights on the antiradical capacity and mechanism of phytocannabinoids: H-abstraction and electron transfer processes in physiological media and the influence of the acid-base equilibrium, *Phytochemistry*, 2023, **208**, 113608, DOI: 10.1016/j.phytochem.2023.113608.

43 M. E. Alberto, N. Russo, A. Grand and A. Galano, A physicochemical examination of the free radical scavenging activity of Trolox: mechanism, kinetics and influence of the environment, *Phys. Chem. Chem. Phys.*, 2013, **15**(13), 4642–4650, DOI: 10.1039/C3CP43319F.

44 H. Boulebd, Radical scavenging behavior of butylated hydroxytoluene against oxygenated free radicals in physiological environments: Insights from DFT calculations, *Int. J. Chem. Kinet.*, 2022, **54**(1), 50–57, DOI: 10.1002/kin.21540.

45 Z. Li, G. Sun, M. Chen, S. Jin, X. Hao, C. Zhang, J. Ouyang, J. Zhu, B. Li, F. Cheng and Y. Xue, Evaluation of the radical scavenging potency and mechanism of natural phenolamides: A DFT study, *J. Mol. Liq.*, 2023, **383**, 122140, DOI: 10.1016/j.molliq.2023.122140.

46 R. Castañeda-Arriaga, T. Marino, N. Russo, J. R. Alvarez-Idaboy and A. Galano, Chalcogen effects on the primary antioxidant activity of chrysin and quercetin, *New J. Chem.*, 2020, **44**(21), 9073–9082, DOI: 10.1039/D0NJ01795G.

47 Q. V. Vo, N. T. Hoa, N. M. Thong and A. Mechler, The hydroperoxyl and superoxide anion radical scavenging activity of anthocyanidins in physiological environments: Theoretical insights into mechanisms and kinetics, *Phytochemistry*, 2021, **192**, 112968, DOI: 10.1016/j.phytochem.2021.112968.

48 H. Boulebd, A. Mechler, N. Thi Hoa and Q. V. Vo, Insights on the kinetics and mechanisms of the peroxyl radical scavenging capacity of caftaric acid: the important role of the acid–base equilibrium, *New J. Chem.*, 2022, **46**(16), 7403–7409, DOI: 10.1039/D2NJ00377E.

49 S. Hippeli and E. F. Elstner, Transition metal ion-catalyzed oxygen activation during pathogenic processes, *FEBS Lett.*, 1999, **443**(1), 1–7, DOI: 10.1016/S0014-5793(98)01665-2.

50 K. Jomova, S. Baros and M. Valko, Redox active metal-induced oxidative stress in biological systems, *Transition Met. Chem.*, 2012, **37**(2), 127–134, DOI: 10.1007/s11243-012-9583-6.